Proceedings of the ASME 2020 39th International Conference on Ocean, Offshore and Arctic Engineering
OMAE2020
June 28 - July 3, 2020, Fort Lauderdale, USA

OMAE2020-19128

BLOWING THE TOP ON PARAMETRIC RESONANCE - RELIEF VALVE CONTROL FOR THE STABILISATION OF AN OWC SPAR BUOY

Josh Davidson*
Dept of Fluid Mechanics
Faculty of Mechanical Engineering
Budapest Univeristy of Technology and Economics
Email: davidson@ara.bme.hu

Rui P. F. Gomes
IDMEC, Instituto Superior Técnico
Universidade de Lisboa
Av. Rovisco Pais 1, 1049-001 Lisboa, Portugal

Roberto Galeazzi
Dept of Electrical Engineering
Technical University of Denmark
Lyngby DK-2800, Denmark

João C. C. Henriques
IDMEC, Instituto Superior Técnico
Universidade de Lisboa
Av. Rovisco Pais 1, 1049-001 Lisboa, Portugal

ABSTRACT

An active control method, to suppress the onset of pitch/roll parametric resonance on an oscillating water column (OWC) spar buoy, is proposed in this paper, which utilises a pressure relief valve at the top of the OWC air chamber. The paper examines the hypothesis that by opening the relief valve, to reduce the air chamber pressure difference and to decouple the dynamics of the spar buoy and the OWC within, the natural pitch/roll frequencies of the system will be shifted, allowing parametric resonance to be cancelled when its onset is detected. The paper reports on experiments, performed to test the stated hypothesis, with a small-scale model OWC spar buoy in a wave flume. Two configurations are considered and tested in a range of monochromatic waves (1) fully closed air chamber; (2) fully open chamber. The results partially confirm the hypothesis, demonstrating that the occurrence of parametric resonance observed for certain wave frequencies when the chamber is closed does not occur when the chamber is open. However, the change in the natural pitch/roll frequencies between the two configurations is very small, and parametric resonance occurs in both confurations for waves with twice this frequency.

1 INTRODUCTION

An oscillating water column (OWC) spar buoy, is a type of wave energy converter (WEC) that utilises the relative heave motion between an outer spar hull and an inner moonpool-like water column to drive the air, enclosed in a chamber above the OWC, through a turbine at the top of the buoy connected to the atmosphere. Like many offshore spar structures [1–4], this device is prone to large amplitude pitch and roll motions, caused by parametric resonance, when the frequency of the wave is around twice the pitch/roll natural frequency. Parametric resonance is a dynamic instability caused by the time-varying changes in the parameters of a system [5], which manifests in floating offshore structures, due to the wave induced heave motion of the structure varying the metacentric height.

The occurrence of parametric resonance in the OWC spar buoy severely reduces the heave motion and thus energy capture. In addition, the large unstable pitch/roll motions can lead to structural and safety issues. Therefore, parametric resonance is a key problem to be addressed and mitigated in the design of this type of WEC.

*Address all correspondence to this author.

1.1 Parametric resonance in spar type WECs

The concept of resonance is well known in WEC research and development, since maximum energy extraction is typically achieved when the WEC natural frequency matches the peak frequency of the input wave field. By comparison, parametric resonance has received very little attention, probably due to the complexity of the numerical models required to capture this nonlinear phenomenon, compared to the conventional linear/frequency domain models favoured in WEC research and analysis. However, in recent years there has been an increased interest towards modelling and control of parametric resonance in WECs [6], inline with the number of reported observations of parametric instabilities during physical wave tank experiments and the rise of computationally efficient nonlinear hydrodynamic models capable of simulating the occurrence of parametric resonance [7].

Spar type WECs tend to comprise two heaving bodies, extracting energy through their relative motion. Parametric instability in the pitch/roll degrees of freedom (DoFs) for these devices have been observed experimentally [8–10] and numerically [11, 12]. The OWC spar buoy also consists of two heaving bodies, the outer spar buoy and the inner OWC. The experimental and numerical observations of parametric instability for this device is reviewed in Section 2.

A small number of studies have made initial attempts towards reducing parametrically excited pitch/roll motions in spar-type WECs, through the use of passive mechanisms, such as fins or strakes, to increase the hydrodynamic damping in the pitch/roll DoFs. This approach has been shown to reduce the occurrence of parametric resonance in conventional spar platforms [2]. The use of strakes is numerically investigated in [9], after experimental testing of *WaveBob*-like, two-body heaving point absorbers, revealed that power production is limited by the excessive pitch and roll motions when parametric resonance occurs. The simulation results confirm the ability of the strakes to reduce pitch and roll amplitudes, allowing increased WEC power output. The use of fins has been investigated for the stabilisation of the OWC spar buoy in [13], as discussed in Section 2.

1.2 Objective and outline of paper

The present paper proposes an active control method, to counteract the development of parametric resonance on the OWC spar buoy, based on the hypothesis that opening a pressure relief valve in the OWC air chamber can shift the frequency response of the device dynamics, thereby detuning the frequency coupling responsible for the existence of parametric resonance. Section 2 reviews the occurrence of parametric resonance in the OWC spar buoy and introduces the proposed control method. Next, in Section 3, the paper reports on experiments, performed to test the stated hypothesis, with a small-scale model OWC spar buoy in a wave flume. The results are presented in Section 4 and then conclusions are drawn in Section 5.

2 PARAMETRIC RESONANCE IN THE OWC SPAR BUOY

Fig 1 presents a schematic view of an OWC spar buoy, as well as a photo from a prototpye model used for testing.

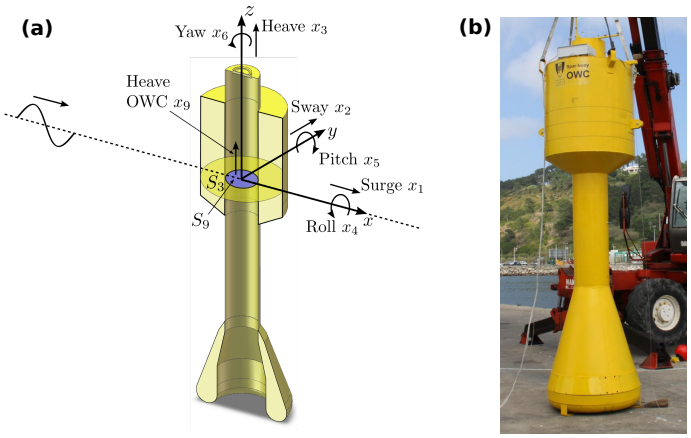

FIGURE 1: (a) Cut section view of an OWC spar buoy with indication of the fixed reference frame and oscillation modes (from [14]). (b) The 1:16 scale OWC spar buoy model (from [15]).

2.1 Dynamic instability

The dynamic instability of the OWC spar buoy has been noted and reported in a number of studies at various scales. It was first reported in [16] from a 1:120 scale testing of the device at the wave flume in Instituto Superior Técnico, Lisbon, Portugal. Further tests at the same scale are shown in [17, 18], where the experimental results are compared against linear models, and large differences between the numerical and experimental results are observed for the pitch motion at twice the natural frequency due to parametric resonance. Further experiments are performed in the same wave flume at 1:100 scale in [13], for the purpose of testing a passive control scheme to reduce the parametric resonance, shown in Fig. 2. A 1:16 scale OWC spar bouy, shown in Fig 1, was tested at the large scale wave flume of NAREC (Blyth, United Kingdom), where pitch and roll parametric resonance was observed and drastically reduced the power conversion performance [15].

In addition to the experimental observations, the occurrence of parametric resonance in the OWC spar buoy has also been noted in a number of numerical studies. To test the ability of a computationally efficient nonlinear hydrodynamic modelling technique to capture parametric resonance, the 1:100 scale OWC spar buoy from [13] is used as a case study in [12] and the simulations predict the large amplitude parametric pitch and roll motions at the expected frequencies. The same modelling technique

is then applied to the 1:16 scale OWC spar bouy from [15] to investigate the effect of mooring parameters on the dynamic instability in [19], where it is concluded that the parametric roll response is found to have little dependence on different mooring configuration tested. A procedure to identify the frequency and ampitude ranges in which parametric resonance will occur is included into the numerical optimization routines in [14] and a penalty added to these configurations, due to the decreased performance when parametric resonance occurs.

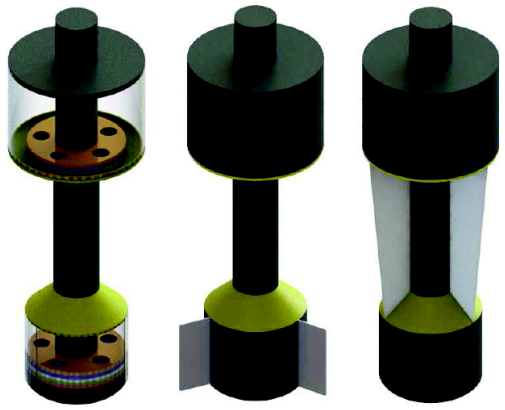

FIGURE 2: The addition of fins to the OWC spar buoy model as a passive control strategy in [13]. (a) Is the original geometry, (b) and (c) have three equally-spaced fins installed on the bottom tube and between the floater and the bottom tube, respectively.

2.2 PROPOSED RELIEF VALVE CONTROL

The present paper proposes an active control method to reduce the occurrence of large roll/pitch amplitudes induced by parametric resonance through the opening or closing of the air chamber relief valve. The paper examines the hypothesis that by opening the relief valve, to reduce the air chamber pressure difference and to decouple the dynamics of the spar buoy and the oscillating column of water within, the roll and pitch natural frequencies of the system will be shifted, allowing parametric resonance in these DoFs to be cancelled when its onset is detected.

2.2.1 Inspiration from a similar case Villegas and van der Schaaf consider the two body, self-reacting, heaving point absorber, the *WaveBob* [8]. Similar to the present case, parametric pitch/roll was detected in physical experiments, to the detriment of the WEC performance. An active control system to mitigate the occurrence of parametric resonance is proposed. The control system acts on the WEC dynamics, through the effect of the PTO force between the two bodies. The PTO force, couples the motion of the two bodies, influencing the resonant peaks in the frequency response of the heave, pitch and roll DoFs. The active control system proposed by Villegas and van der Schaaf, applies a notch filter, designed to eliminate any PTO forces at the frequencies for which parametric resonance occurs. Experimental results for a model scale device in a wave tank validate the effectiveness of this approach in [8]. A number of similarities can be noted between the *WaveBob* and the OWC spar buoy: they are both two-body spar buoy systems, where the heave motion of the bodies are coupled through the PTO. For the OWC the PTO damping is determined by the size and rotational speed of the turbine. Increasing the rotational speed or reducing the turbine size has the effect of increasing the turbine damping. The use of a relief valve in parallel with the turbine has the consequence of reducing the overall turbine damping. Therefore, opening a valve ('blowing the top') on the OWC chamber, has the same effect as the notch filter in [8].

2.2.2 Supporting evidence from other cases Further confidence to this strategy is provided by additional studies uncovered during the literature review for this paper. [20] experimentally tested a floating cylindrical OWC, considering five different orifice diameters in the OWC. Interestingly, extremely large amplitude roll motions, at twice the natural roll fequency, occur for one orifice diameter. For the other orifice diameters at this frequency, two had slightly larger than normal roll amplitudes, and the other two had normal roll amplitudes, compared to the amplitude trend of surrounding frequencies. This suggests that the occurrence of parametric resonance might be dependent on, and therefore controlled by, the OWC damping.

The experiments in [21] aim to provide numerical validation for linear hydrodynamic models developed for a free-floating sloped WEC. This device has a fully submerged tube attached to a buoy, inclined at an angle and open to the sea at both ends. The water inside the tube tends to remain stationary while the buoy moves in response to input waves. Thus power can be extracted from the relative motion between the water inside the tube and the oscillating buoy, using a piston inside the tube. Experiments were performed with the tube open and with the tube blocked. Since the device is symmetric with respect to the incoming waves, the linear models predicted no motion in the roll DoF, however, significant roll motions are observed at a certain range of frequencies due to parametric resonance. Interestingly, there is a shift in the frequencies for which parametric resonance occurred between the open and blocked tube configurations, with the peaks occurring at 0.85 and 0.78 Hz, respectively.

3 EXPERIMENTS

The experiments are performed using the same model OWC Spar Buoy and wave flume as in [13]. Section 3.1 describes the experimental setup and Section 3.2 details the series of tests.

3.1 Experimental setup

The experiments are conducted at the wave flume in Instituto Superior Técnico, Lisbon, Portugal, which is 20 m long and 0.7 m wide. A water depth of 0.5 m was used. The flume is equipped with a HR Wallingford wave generation system with a piston-type wavemaker with active absorption of reflected waves and a constant-slope dissipative beach at opposite end of the flume. A schematic of the experimental setup is shown in Fig 3.

The OWC spar buoy model is the original geometry, without fins, used in [13]. The model geometry is based on the optimized geometry of the OWC spar buoy [22], with comparable diameter, draft and mass distribution, with the exception that the models inner tube has a uniform cross-section. The full characteristics of the model are documented in [13]. Two different configurations of the model are used in the present experiments: (1) Closed OWC - where the top of the OWC chamber is sealed closed and no air flow is possible, and (2) Open OWC - where the top of the OWC chamber is fully open (seen in Fig 4 (b)).

The model is kept on station using a three-line, slack-mooring system, as illustrated in Fig 3, which is designed to produce a negligible influence on the heave dynamics. Each individual line is composed of three line-segments with a clump weight and a float at the connection points. The fairleads are located at the free surface. Ideally, the three fairleads should be equally-spaced in the circumferential direction, with an angle of 120 deg between them. Since the channel dimensions do not allow it, the angle between the two lines on the leeward (α) was set to 29 deg. Although the same mooring configuration is applied as in [13], the mooring system was re-made using new lines, thus there is less confidence that the characteristics of the mooring system are exactly the same (as was the case for the model geometry), with possibilities of the clump weights, floaters or anchor weights being located in slightly different positions.

The motion of the floating model, in 6-DoF, is captured using a Qualisys motion tracking system, comprising a system of infrared cameras that captures the motion of reflective markers attached to the model (seen on the top of the model in Fig 4). The free surface elevation (FSE) is measured with ultrasonic sensors at two different locations, next to the model(X_1) and in front of the model (X_2), as displayed in Fig. 3. Both body motion and FSE are sampled at 100Hz. The pressure difference between the air chamber and the exterior atmosphere is measured, by a differential pressure sensor, connected to the model by a low weight tube appendage (seen on the top of the model in Fig 4). However, the pressure measurements are not used in the present paper.

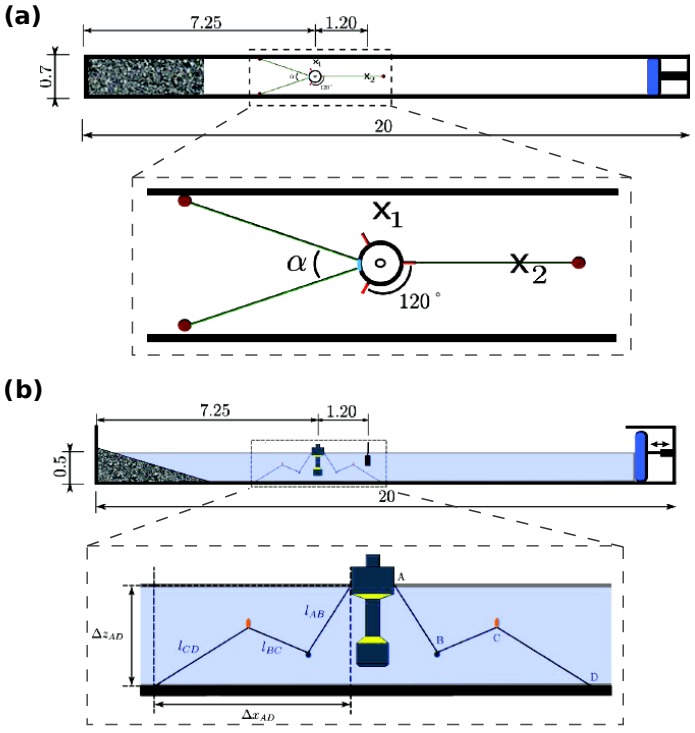

FIGURE 3: Schematic representation of the wave channel and of the OWC spar buoy model and its mooring system: (a) top view with a detail view of the model; (b) side view with a detail view of the model. (from [13]).

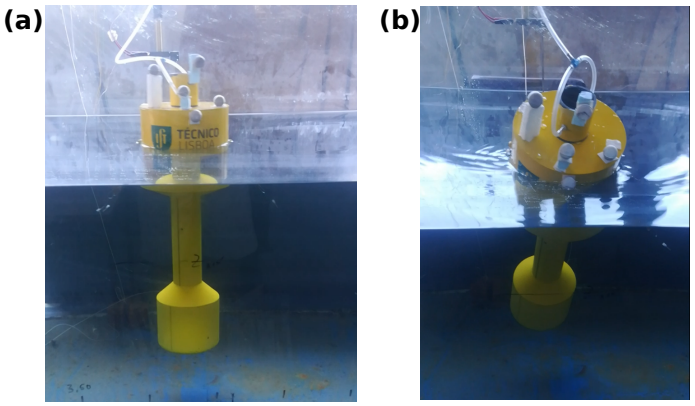

FIGURE 4: Photo of the model OWC spar buoy, including the reflective markers for motion tracking and the tube appendage for pressure measurement. (a) At its equilibrium position. (b) During large amplitude parametric roll motion (here the opened top of the OWC can be seen).

3.2 Tests

Two sets of tests are performed in the wave flume: free decay and wave induced motion experiments.

3.2.1 Free decay The free decay experiments are performed to determine the natural frequencies of the heave, pitch and roll DoFs. Although for an axisymmetric device, the pitch and roll DoFs should theoretically be identical, the air tubes attached to the OWC chamber for measuring the air pressure, are aligned to minimise any influence in the pitch DoF, but appear to perhaps add a small amount of stiffness in the roll DoF. Therefore, both pitch and roll DoFs are tested separately. The model is manually displaced from its equilibrium and then released, with the resulting body motion being measured until the model comes to rest. The experiment is performed three times for each DoF, for both the Open and Closed OWC. Results are shown in Section 4.1.

3.2.2 Wave induced motion To compare the frequency response of the Open and Closed OWCs, a series of experiments utilising monochromatic waves with a range of frequencies are performed. A total of 27 different frequencies, spanning 0.4 - 1.3Hz are tested, with a higher resolution around the frequencies where parametric resonance is observed. The target wave amplitude is 0.01m, and each experiment is 120s in duration. The waves are initially generated and measured in an empty tank (without the model in place), and the results are presented in Section 4.2.1. Next, the Closed OWC model is placed in the tank and the resulting body motions measured for the series of input waves. Then the top is removed from the model and the Open OWC is tested, with the results presented in Section 4.2.

4 RESULTS

The results of the free decay tests are presented in Section 4.1 and the wave induced motion tests in Section 4.2.

4.1 Free Decay

The results of the free decay tests are plotted in Fig. 5, showing the start of the recorded time series for the three heave, pitch and roll experiments, for both the Open and Closed OWCs. Additionally, the frequency spectrum for each of the time series is shown. To calculate the spectra, a fast Fourier transform (FFT) is used, and zero padding is added to the end of the free decay time signal to increase the resulting frequency resolution.

The natural frequencies of the heave, pitch and roll DoFs are calculated using the peak of the spectra plotted in Figs 5 (c),(f) and (i), respectively, and confirmed by measuring the period between successive peaks in the time series. The results are recorded in Table 1.

Fig 5 (a)-(c) show the heave free decays. A number of differences can be noted between the Open and Closed OWCs:

1. The equilibrium level for the Open OWC is lower. The entrapped air for the Closed OWC allows the buoy to float at a higher level.
2. The natural frequency of the devices is different. The peak frequencies of the free decay spectra show that the Open OWC has a higher natural frequency than the Closed OWC. This could be expected, considering the added inertia in the Closed OWC from the water column, that is not as strongly coupled to the body for the Open OWC, which would decrease the natural frequency of the Closed OWC.
3. The Open OWC has a second smaller peak at 1.04 Hz. This is due to the dynamics of the water column, since two-body systems can have twin peaks in their spectra. For the Closed OWC, the motion of the water column and body are locked together, resulting in a single peak between the twin peaks of the Open OWC. This type of behaviour is also noted in [8] for the case of large damping in the *WaveBob* PTO. For the Closed OWC, the closed orifice equates to infinite damping.

The lower equilibrium level (increased submergence) for the Open OWC means that the position of the centre of buoyancy is also lower, which would change the hydrostatic restoring torque coefficient, and thus shift the natural frequency in pitch and roll. Indeed, this shift in natural frequency is observed in Figs 5 (f) and (i), however, the change is relatively small. Table 1 shows that the natural pitch frequency is 0.39 Hz for the Closed OWC and 0.40 Hz for the Open OWC, and the natural roll frequency is 0.38 Hz for the Closed OWC, and 0.39 Hz for the Open OWC. Thus the change in natural frequency is only about 2.5%. The shift of the resonance to a lower frequency for the closed case, compared to the open case, agrees with the results found in [21].

		Test 1	Test 2	Test 3	Average
Heave	**Open**	1.156	1.161	1.167	1.16
	Closed	1.070	1.078	1.087	1.08
Pitch	**Open**	0.403	0.404	0.404	0.40
	Closed	0.395	0.395	0.394	0.39
Roll	**Open**	0.389	0.389	0.389	0.39
	Closed	0.382	0.382	0.381	0.38

TABLE 1: Natural frequency (in Hz) for the heave, pitch and roll DoFs, determined from the free decay experiments.

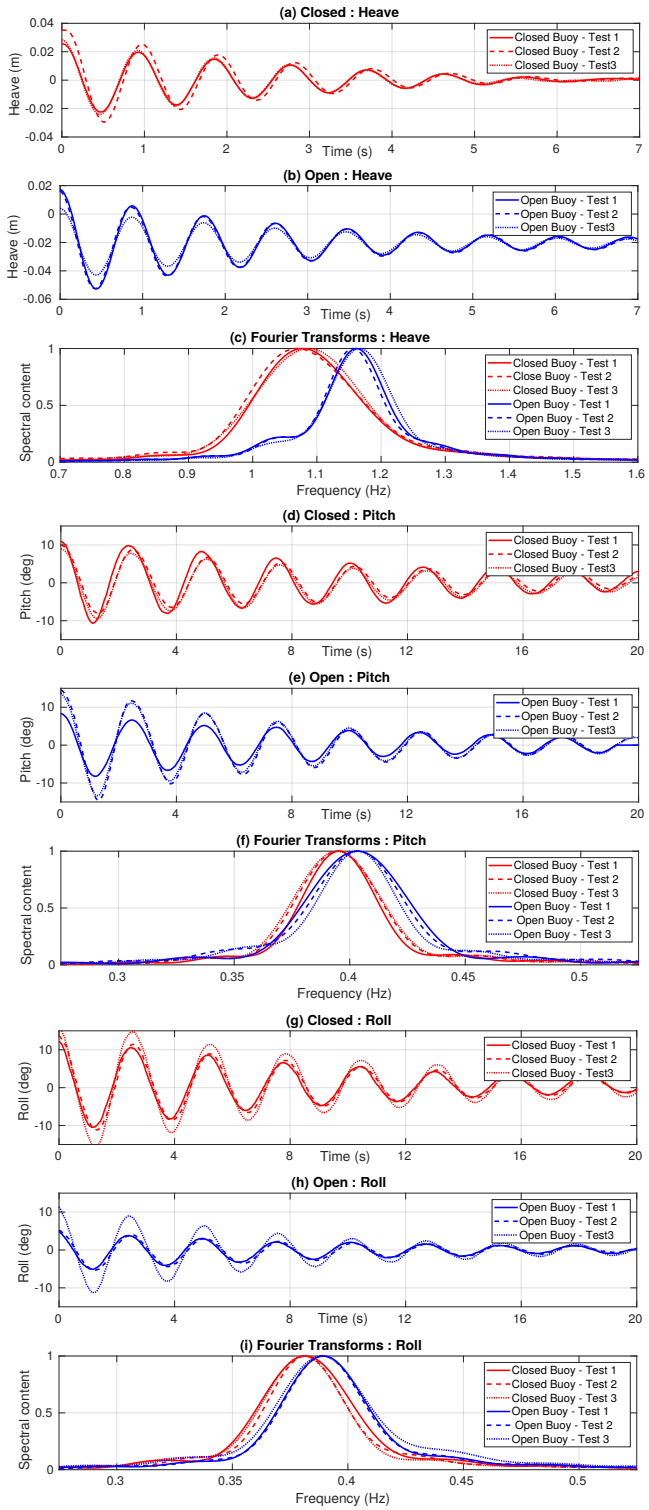

FIGURE 5: The free decay time series (a,b,d,e,g and h) and their power spectra normalised against the peak value (c,f and i).

4.2 Wave induced motion

The analysis of the wave induced motion begins in Section 4.2.1, by examining the input waves used for the experiments. Next, the resulting time series of body displacements are presented in Section 4.2.2. Due to a large number of tests (27 different frequencies), only a subsection of the results can be shown. However, the important information is condensed into a form which can be easily displayed and interpreted, through the maximum displacement at each frequency (Section 4.2.3) and a frequency domain analysis (Section 4.2.4).

4.2.1 Wave generation

Although a target wave amplitude of 0.01m was set, the wavemaker does not perform equally at all frequencies. Figs 6 (a) and (b) plot the measured FSE for the 0.4 Hz and 1 Hz waves, respectively, showing the amplitude at 0.4 Hz more than doubles that at 1 Hz. Therefore, the amplitude at each frequency is calculated, taking the average of the maximum and minimum FSE between each zero crossing, using the last quarter of the time series, plotted in Fig. 6(c).

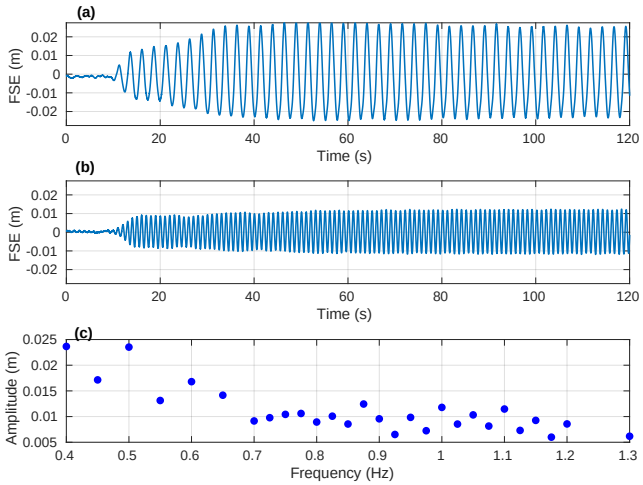

FIGURE 6: Measured FSE for the (a) 0.4 Hz and (b) 1 Hz wave. (c) Average wave amplitude at each frequency tested.

4.2.2 Body motion - Time series

Fig. 7 plots results of the heave, pitch and roll displacements for the Open and Closed OWCs. Due to space constraints, only three example frequencies are shown, 0.4, 0.8 and 1 Hz. In Figs. 7 (a)-(c), the large amplitude motion at 0.4 Hz is due to the large amplitude input wave at this frequency (see Fig 6). The amplitude of the pitch motion is additionally influenced by resonance, since 0.4 Hz corresponds to the natural frequency of the pitch DoF. Although the roll natural frequency is also 0.4 Hz, there is no direct wave excitation of the roll DoF for an axisymmetric body, thus the amount of roll motion is much less than the other DoFs.

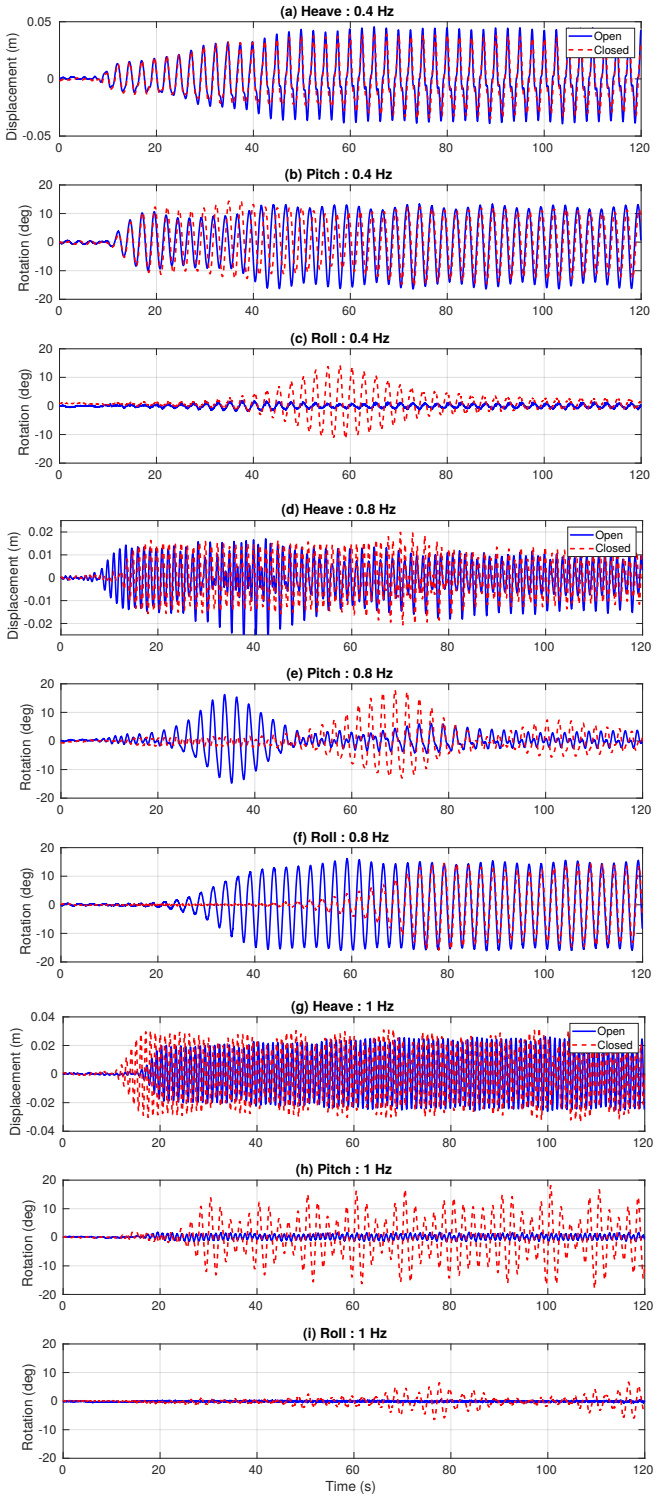

FIGURE 7: The measured heave (a,d and g), pitch (b,e and h) and roll (c,f and i) displacements for three different wave frequencies.

For the 0.8 Hz wave, parametric pitch and roll motion can be observed in Figs 7 (e) and (f), identifiable since the oscillations are at half the frequency of the heave motion in Fig. 7-(d). This frequency equals twice the natural frequency of the pitch and roll modes of motion, thus parametric resonance is expected if the heave motion exceeds a certain threshold. The parametric motion is observed to transfer between the pitch and roll modes. In the case of the 1 Hz wave, parametric resonance can be observed for the Closed OWC but not for the Open OWC. Although the amplitude of the parametric resonance in Figs 7 (e), (f) and (h) appear to be of similar amplitude to the normal resonance case in 7 (b), it should be noted that the input wave amplitude is twice as high for the 0.4 Hz case.

4.2.3 Body motion - Maximum displacement

To compare the maximum response at each frequency, the displacements are first normalised against the corresponding wave amplitude for that frequency. The normalised maximum displacements at each frequency, for the three DoFs, are plotted in Fig. 8. Comparing the Open and Closed OWCs, it can be seen that both exhibit large pitch and roll motions, of similar amplitude, around twice the natural frequency of these DoFs (0.8 Hz). However, for frequencies higher than this, the pitch and roll amplitudes of the Closed OWC remain large, and are always bigger than those of the Open OWC, which rapidly decrease to non-resonant amplitudes. The pitch amplitude of the Open OWC are seen to increase again around the natural heave period, where the heave amplitudes are observed to be large.

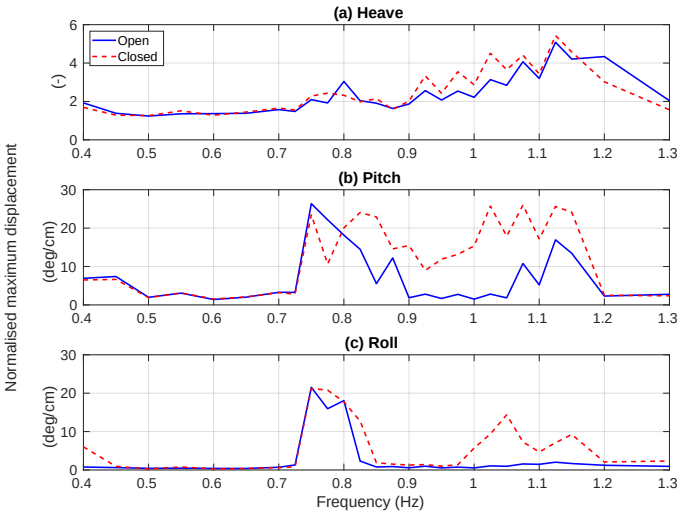

FIGURE 8: The maximum displacement for heave, pitch and roll, at each frequency, normalised against the wave amplitude

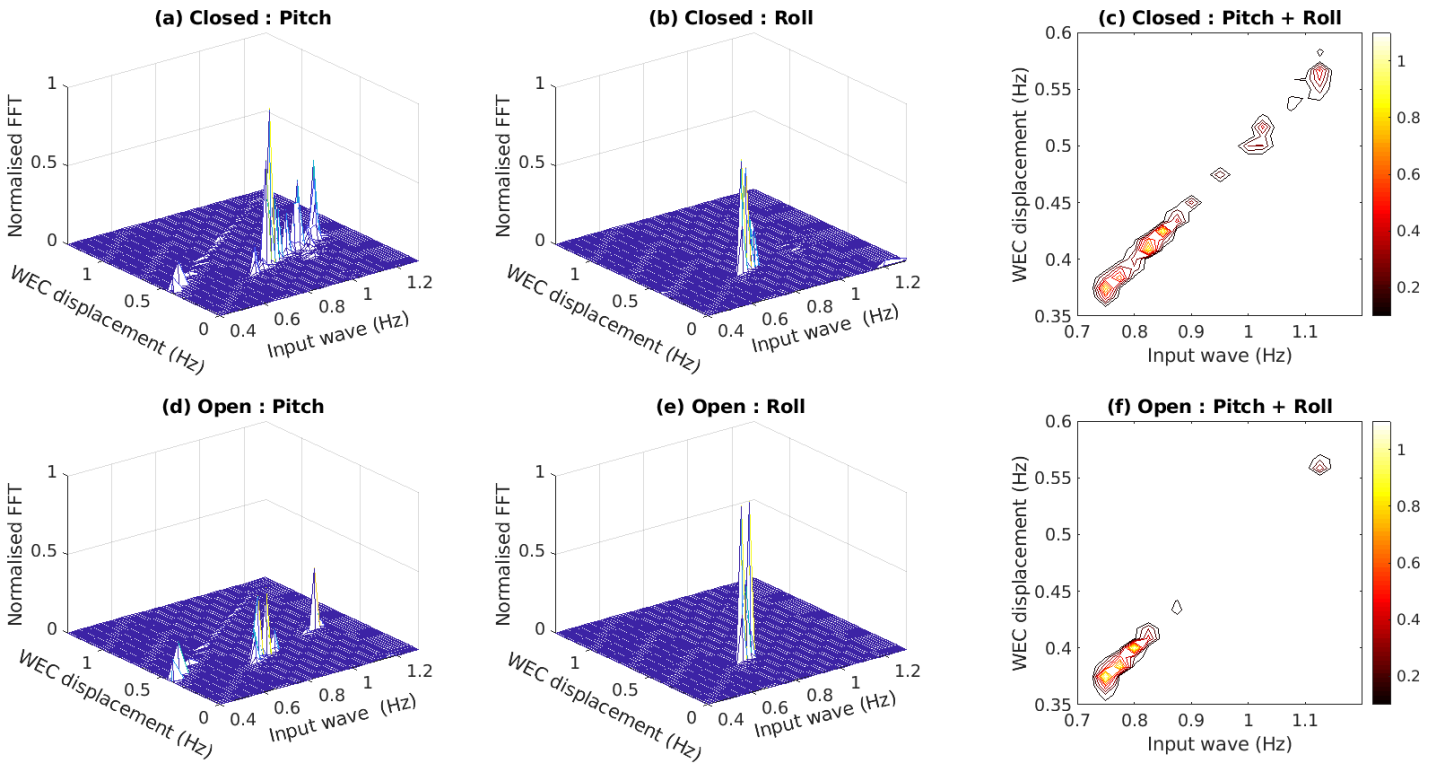

FIGURE 9: The frequency domain results for the Open (a-c) and Closed (d-f) OWCs. The FFT of the (wave amplitude normalised) pitch time series, for each of the tested input wave frequencies, are shown in (a) and (d). Similarly, the results for roll are shown in (b) and (e). To simplify the comparison, the FFT values in these plots are normalised by the largest value in the four plots. The sum of the pitch and roll normalised FFT values are shown in (c) and (f), zoomed in on the frequency ranges corresponding to parametric resonance.

4.2.4 Body motion - Frequency domain

While the maximum displacements provide a decent metric to judge the ability of the Open OWC to influence the prevalence of parametric resonance (compared to the Closed OWC), performing an FFT on the time series and observing the location and amplitude of the spectral peaks offer two additional insights:

1. Location - The key signature of parametric resonance is a period-doubling compared to the input oscillations. This can be manually observed and verified in Figs 7 (e), (f) and (h). However, in the frequency domain, the location of the peaks give an automatic verification whether the frequency of the pitch/roll motions is half the input wave frequency.
2. Amplitude - The amplitude of the frequency response is a measure of the energy in the time domain signal. It can, therefore, indicate the relative duration for which large amplitude motions occur. For example, consider the pitch and roll motions at 0.8 Hz, in Figs 7 (e) and (f). The maximum displacement for the four time series is nearly identical. However, this maximum amplitude only occurs for one or two periods in pitch, but for over 20 periods in roll, and for much longer in the Open OWC than in the Closed OWC.

Fig 9 displays the frequency domain information, obtained by performing an FFT on the body motion time series to give the WEC displacement power spectra for each of the 27 different input wave frequencies. The pitch results are plotted in Figs 9 (a) and (d), where the large peaks from parametric resonance can be seen occuring with the WEC displacement frequency being half of the input wave frequency. Also seen in the plot is a second smaller ridge of peaks running diagonally across the plot, where the WEC displacement frequency equals the input wave frequency, corresponding to normal wave-driven motion. This second smaller ridge of peaks does not appear in Figs 9 (b) and (e), since there is no direct wave excitation for the roll DoF in an axisymmetric body. However, large amplitude peaks due to parametric resonance can be seen for the roll motion.

Figs 9 (c) and (f) provide a visual means to best compare the occurrence of parametric resonance in the Open and Closed OWC's, by displaying a contour plot of the total energy parametrically transferred to pitch and roll. As shown in Figs 7 (e) and (f), the parametric motion can transfer between pitch and roll, so it is important to consider them together when assessing the occurrence of parametric resonance. Comparing plots in Figs 9 (c)

and (f), it can be observed that the Open OWC is able to reduce the range of frequencies for which parametric resonance occurs.

5 CONCLUSION

The paper proposed utilising a pressure relief valve in the chamber of the OWC spar buoy as a control mechanism to detune the frequency coupling responsible for the existence of parametric resonance. The results from the model scale experiments showed that the effect of opening a relief valve on the natural pitch and roll frequencies was small, but more significant on the natural heave frequency. In monochromatic waves, for the amplitude tested, by shifting the heave resonance further away from the frequency region where parametric pitch and roll motions are observed, the opened relief valve is able to reduce the frequency range where parametric resonance occurs.

ACKNOWLEDGMENT

This project has received funding from the European Union's Horizon 2020 research and innovation programme under the Marie Sklodowska-Curie grant agreement No 867453. The present research work was also partially funded by the Portuguese Foundation for Science and Technology (FCT), through IDMEC, under LAETA project UID/EMS/50022/2019.

REFERENCES

[1] Koo, B., Kim, M., and Randall, R., 2004. "Mathieu instability of a spar platform with mooring and risers". Ocean engineering, **31**(17), pp. 2175–2208.

[2] Rho, J. B., Choi, H. S., Shin, H. S., Park, I. K., et al., 2005. "A study on mathieu-type instability of conventional spar platform in regular waves". International Journal of Offshore and Polar Engineering, **15**(02).

[3] Neves, M. A., Sphaier, S. H., Mattoso, B. M., Rodriguez, C. A., Santos, A. L., Vileti, V. L., and Torres, F., 2008. "On the occurrence of mathieu instabilities of vertical cylinders". In Proc. of the 27th International Conference on Offshore Mechanics and Arctic Engineering,.

[4] Jang, H., and Kim, M., 2019. "Mathieu instability of arctic spar by nonlinear time-domain simulations". Ocean Engineering, **176**, pp. 31–45.

[5] Fossen, T., and Nijmeijer, H., 2011. Parametric resonance in dynamical systems. Springer.

[6] Davidson, J., Kalmar-Nagy, T., Giorgi, G., and Ringwood, J. V., 2018. "nonlinear rock and roll–modelling and control of parametric rresonances in wave energy devices". In Proc. 9th Vienna Int. Conf. Math. Modelling.

[7] Davidson, J., and Costello, R., 2020. "Efficient nonlinear hydrodynamic models for wave energy converter design - a scoping study". Journal of Marine Science and Engineering.

[8] Villegas, C., and van der Schaaf, H., 2011. "Implementation of a pitch stability control for a wave energy converter". In Proceedings of the 10th European Wave and Tidal Energy Conference, Southampton, UK.

[9] Beatty, S. J., Roy, A., Bubbar, K., Ortiz, J., Buckham, B. J., Wild, P., Stienke, D., and Nicoll, R., 2015. "Experimental and numerical simulations of moored self-reacting point absorber wave energy converters". In The Twenty-fifth International Ocean and Polar Engineering Conference.

[10] Kurniawan, A., Grassow, M., and Ferri, F., 2019. "Numerical modelling and wave tank testing of a self-reacting two-body wave energy device". Ships and Offshore Structures, pp. 1–13.

[11] Tarrant, K., and Meskell, C., 2016. "Investigation on parametrically excited motions of point absorbers in regular waves". Ocean Engineering, **111**, pp. 67–81.

[12] Giorgi, G., and Ringwood, J. V., 2018. "Articulating parametric resonance for an owc spar buoy in regular and irregular waves". Journal of Ocean Engineering and Marine Energy, **4**(4), pp. 311–322.

[13] Gomes, R., Malvar Ferreira, J., Ribeiro e Silva, S., Henriques, J., and Gato, L., 2017. "An experimental study on the reduction of the dynamic instability in the oscillating water column spar buoy". In Proceedings of the 12th European Wave and Tidal Energy Conference, Cork, Ireland.

[14] Gomes, R., Henriques, J., Gato, L., and Falcao, A., 2019. "An upgraded model for the design of spar-type floating oscillating water column devices". In 13th European Wave and Tidal Energy Conference.

[15] Gomes, R., Henriques, J., Gato, L., and Falcão, A., 2018. "Experimental tests of a 1: 16th-scale model of the spar-buoy owc in a large scale wave flume in regular waves". In ASME 2018 37th International Conference on Ocean, Offshore and Arctic Engineering.

[16] Gomes, R., Henriques, J., Gato, L., and Falcao, A., 2012. "Testing of a small-scale floating OWC model in a wave flume". In International Conference on Ocean Energy, pp. 1–7.

[17] Gomes, R., Henriques, J., Gato, L., and Falcão, A. d. O., 2015. "Wave channel tests of a slack-moored floating oscillating water column in regular waves". In Proceedings of the 11th European Wave and Tidal Energy Conference, Nantes, France, pp. 6–11.

[18] Gomes, R., Henriques, J., Gato, L., and Falcão, A., 2020. "Time-domain simulation of a slack-moored floating oscillating water column and validation with physical model tests". Renewable Energy, **149**, pp. 165–180.

[19] Giorgi, G., Gomes, R., Bracco, G., and Mattiazzo, G., 2020. "The effect of mooring line parameters in inducing parametric resonance on the spar-buoy oscillating water

column wave energy converter". Journal of Marine Science and Engineering, **8**(1).

[20] Sheng, W., Flannery, B., Lewis, A., and Alcorn, R., 2012. "Experimental studies of a floating cylindrical owc wec". In ASME 2012 31st International Conference on Ocean, Offshore and Arctic Engineering.

[21] Payne, G. S., Taylor, J. R., Bruce, T., and Parkin, P., 2008. "Assessment of boundary-element method for modelling a free-floating sloped wave energy device. part 2: Experimental validation". Ocean Engineering, **35**(3-4), pp. 342–357.

[22] Gomes, R., Henriques, J., Gato, L., and Falcão, A., 2012. "Hydrodynamic optimization of an axisymmetric floating oscillating water column for wave energy conversion". Renewable Energy, **44**, pp. 328–339.